# On the Nature of the Fluorescent State in β-Nitrotetraarylporphyrins

**Vladimir S. Chirvony,[†] Arie van Hoek,[‡] Tjeerd J. Schaafsma,*[,‡] Petr P. Pershukevich,[†] Igor V. Filatov,[†] Igor V. Avilov,[†] Svetlana I. Shishporenok,[†] Sergei N. Terekhov,[†] and Vladimir L. Malinovskii[§]**

*Institute of Molecular and Atomic Physics, National Academy of Sciences of Belarus, F. Skaryna Ave. 70, Minsk 220072, Belarus; Laboratory of Molecular Physics, Department of Biomolecular Sciences, Agricultural University, Dreijenlaan 3, 6703 HA Wageningen, The Netherlands, and A. V. Bogatsky Physico-Chemical Institute, National Academy of Sciences of Ukraine, Lustdorfskaya doroga 86, 270080, Odessa, Ukraine*

*Received: April 28, 1998; In Final Form: September 22, 1998*

2-$NO_2$-5,10,15,20-tetraphenylporphyrin ($H_2TPP-NO_2$) is shown to exist in solution as an equilibrium mixture of two NH tautomers with different spectral and photophysical properties. At 77 K in a rigid glass solution the fluorescence spectra of the tautomers contain two well-resolved narrow bands that are slightly (∼300 $cm^{-1}$) Stokes-shifted with respect to the corresponding $Q_{X00}$ absorption bands, with the spectrum of the more stable tautomer being ∼500 $cm^{-1}$ red-shifted as compared to the spectrum of the less stable tautomer. At room temperature, the tautomers show almost identical broad and structureless fluorescence spectra, markedly red-shifted relative to the longest wavelength absorption band. The Stokes shift increases with an increase of solvent polarity, being as large as ∼2000 $cm^{-1}$ in *N*,*N*-dimethylformamide. Fluorescence lifetimes of the tautomers are found to be markedly (about a factor of 2) different, with both decreasing with an increase of solvent polarity. The reasons for these peculiar fluorescence properties can be understood on the basis of semiempirical quantum chemical calculations. Charge-transfer (CT) states are found to be located between the porphyrinic Q and B states for both tautomers, and a different energy of the CT states gives rise to different fluorescence lifetimes of the tautomers. The calculations also predict a lowering of the $Q_X$ state energy and an increase of its dipole moment $\mu$ with a decrease of the angle $\theta$ between the plane of the $NO_2$ group and the porphyrin plane (relative to the ground-state equilibrium geometry with $\theta = 80°$). We suggest that, in solution, such an increase in the $\mu$ value should result in an increase of the stabilization interaction between the polar porphyrin and solvent molecules and, consequently, in flattening of the $Q_X$ state energy curve as a function of $\theta$ and a shift of the minimum of this curve to $\theta$ values less than 80°. Both quantum chemical calculations and picosecond transient absorption measurements of the $S_1 \rightarrow S_n$ absorption show that the fluorescent $Q_X$ state of $H_2TPP-NO_2$ has mainly $^1(\pi,\pi^*)$ character with a relatively small charge-transfer admixture.

## Introduction

Porphyrins bearing electron-withdrawing substituents are widely used for modeling the primary charge-separation process in photosynthesis. For example, a large number of investigations have been made along this line using relatively simple porphyrin−quinone systems, in which a quinone substituent (electron acceptor) is connected directly to the porphyrin periphery (see, for example, refs 1−4). It was found that, under appropriate redox relationships between porphyrin and quinone, fast intramolecular electron phototransfer occurs from the lowest excited singlet $^1(\pi,\pi^*)$ state of the porphyrin (P) to the quinone (Q). It turned out that the lifetime of this charge-separated state $[P^+-Q^-]$ is only a few picoseconds,[4] due to the short distance between the separated charges, resulting in effective charge recombination. Therefore, such simple porphyrin−quinone dyads are less suitable to produce long-lived charge-separated states. A different line of attack on the problem has made use of molecular triads and even more complex systems, for which the final charge-separation state lives for several microseconds (see, for example, refs 5 and 6). The key to the function of these devices is the two-step electron-transfer sequence that separates electronically and energetically the oxidizing and reducing elements, thereby slowing down charge recombination to the ground state.

In this paper, we report the spectral and photophysical properties of a relatively simple porphyrin system with an electron-withdrawing substituent, i.e., 2-nitro-5,10,15,20-tetraphenylporphyrin ($H_2TPP-NO_2$). Recently, for similar β-nitro-substituted tetraarylporphyrins, unusual fluorescence properties have been reported.[7−10] In particular, it has been shown that these compounds exhibit broad, structureless, significantly Stokes-shifted fluorescence spectra. The Stokes shift was found to increase with an increase of the solvent polarity (dielectric constant). The authors[7−10] have interpreted this fluorescent state as having intramolecular charge-transfer (ICT) character of the $[(P^+)-(NO_2)^-]$ type. It has even been suggested[7,9,10] that the fluorescent state may be of "twisted intramolecular charge-transfer" (TICT) origin, corresponding to full electron transfer from the porphyrin ring to the $NO_2$ group. The lifetimes of

* Corresponding author.
[†] National Academy of Sciences of Belarus. Fax: 375 17 2393064. E-mail: chirvony@imaph.bas-net.by.
[‡] Agricultural University. Phone: +31 317 482634; Fax: +31 317 482725, e-mail: Tjeerd.Schaafsma@MAC.MF.WAU.NL.
[§] National Academy of Science of Ukraine. E-mail: malinovskii@paco.net.

10.1021/jp982039k CCC: $15.00 
Published on Web 11/10/1998

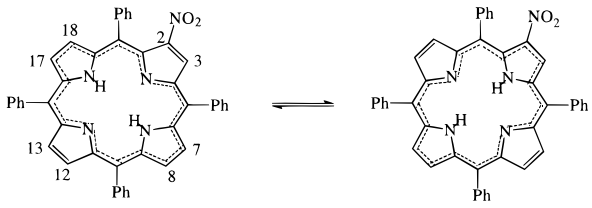


**Figure 1.** Tautomerism of $H_2TPP-NO_2$.

this unusual fluorescence state were found to be in the range of ~1−3 ns.[7−10]

In the present work, we have investigated the $H_2TPP-NO_2$ fluorescent state properties with the aim to elucidate its electronic orbital nature, because, in our opinion, the relatively long lifetime of this state is inconsistent with the suggestion that this state may correspond to full electron transfer from the porphyrin ring to the $NO_2$ group.

A second reason for this work is the possibility for the asymmetrically β-substituted porphyrins to exist in solution as a mixture of two NH tautomers (Figure 1). Indeed, literature data show that 2-nitrotetraphenylporphyrin exists in solution as two equilibrium tautomers that can be distinguished by NMR.[11−13] Effects of the β-nitroporphyrin tautomerism on the optical spectra and the photophysics have not been previously described in the literature, including the above-mentioned work[7,10] on nitroporphyrin free bases.

Note also that in the following we denote the trans tautomer, for which the inner NH protons are located on the pyrroles that do not bear the $NO_2$ substituent, by the term "orthogonal tautomer" (O), whereas the other trans tautomer, for which the HN−NH inner proton axis passes through the pyrrole-bearing $NO_2$ group, is indicated by the term "collinear tautomer" (C).

## Experimental Section

5,10,15,20-Tetraphenylporphyrin ($H_2TPP$) and $H_2TPP-NO_2$ were synthesized and purified following the published methods.[14,15] Absorption spectra were recorded using a Kontron model Uvikon 810 spectrophotometer. Corrected steady-state fluorescence and fluorescence excitation spectra were recorded on a SDL-2 fluorescence spectrometer (LOMO) that measures emission spectra up to 1100 nm. For steady-state fluorescence measurements we used a 90° angle between the excitation and the detection direction.

Time-resolved fluorescence measurements were carried out using a time-correlated photon-counting setup as partly described earlier.[16] A mode-locked continuous wave Nd:YLF laser (Coherent, model Antares 76-YLF) was equipped with an LBO crystal frequency doubler and an BBO crystal as the frequency tripler to obtain up to 1 W of cw mode-locked output power at a 351 nm wavelength. With this UV light a continuous wave dye laser (Coherent Radiation CR590 with extended cavity length) was synchronously pumped. In the dye laser, the dye Coumarine 460 (Exciton Inc.) was used, allowing wavelength tuning from 460 to 510 nm. For the reduction of the pulse rate of excitation pulses to 594 kHz, a setup was used with electrooptic modulators in dual pass configuration, as described earlier.[17] The pulse duration of excitation pulses was ~4 ps full width at half-maximum (fwhm); the maximum pulse energy was ~100 pJ.

Samples were in 0.5 $cm^3$, 1 cm light path fused silica cuvettes. The emission was selected via a polarizer set at the magic angle (54.7°). The fluorescence was collected at an angle of 90° with respect to the direction of the exciting light beam. The filter used for wavelength selection of emission was usually an interference filter combined with an additional cutoff filter. Detection electronics were standard time-correlated single-photon counting modules containing some additional improvements.[18] The instrument response function was ~35 ps fwhm.

For obtaining a dynamic instrumental response as a reference for deconvolution,[19] a reference compound was used with a picosecond single-exponential fluorescence decay. Both Erythrosine B in water and Pinacyanol in ethanol were used for that purpose, depending on the wavelength of detection. Data analysis was performed on a workstation (Silicon Graphics, model Indigo 2), using both the maximum entropy[20] method and the global analysis[21] approach.

Transient absorption spectra were measured by means of a home-built picosecond spectrometer, described in detail in ref 22. Pulses of 25 ps fwhm from a mode-locked $Nd^{3+}$:YAG laser (EKSMA/EKSPLA) were amplified, and the third harmonic (355 nm) was used to excite the sample. The picosecond continuum, used as a probe, was generated in $D_2O$ by the beam of fundamental frequency and delayed with respect to the excitation beam. The transmitted pulses were spectrally resolved and detected by photodiode array polychromators.

All measurements in this work were carried out in solutions containing dissolved oxygen of air. (Note that the air-equilibrated dissolved oxygen should not decrease the corresponding true fluorescence lifetimes and fluorescence quantum yields by more than 10−15%, since $H_2TPP-NO_2$ exhibits fluorescence lifetimes of only a few nanosecond duration.) The porphyrin concentrations used were of $(1-5) \times 0.10^{-5}$ M. For the measurements at 77 K, the mixture toluene/diethyl ether/ethanol (2:2:1, TDE) was used, providing good solubility of the porphyrin as well as good transparent glass at that temperature.

The results of geometry optimization by the semiempirical PM3 method[23] were used as the input geometry of the investigated molecules for calculations of their excited-state properties. The ZINDO/S method[24−26] was used to calculate the positions (wavelengths, $\lambda$) of the $S_0 \rightarrow S_n$ electronic transitions, their oscillator strengths ($f$), dipole moments ($\mu$) in the ground and excited states, and their electronic charge distribution. Up to 121 singly excited configurations were used in the CI procedure. The excited-state property calculations were performed for various angles between the plane of the $NO_2$ group and that of the pyrrole ring of the porphyrin macrocycle.

## Results

**Absorption Spectra.** The absorption spectra of $H_2TPP-NO_2$ in TDE (both at room and liquid nitrogen temperatures) are shown in Figure 2. For a comparison, the room-temperature absorption spectrum of unsubstituted $H_2TPP$, measured at the same porphyrin concentration, is also included in Figure 2. The wavelengths of the major absorption bands of $H_2TPP-NO_2$ in several solvents at room temperature and in TDE at 77 K are listed in Table 1. $H_2TPP-NO_2$ exhibits a typical porphyrinic spectrum with an intense Soret band (B band) followed by four weak Q bands. However, the absorption bands are red-shifted and broadened in $H_2TPP-NO_2$ relative to the unsubstituted $H_2$-TPP. More exactly, the width of the Soret band of $H_2TPP-NO_2$ is about twice the width of $H_2TPP$ (1500 and 690 $cm^{-1}$, respectively, in TDE at room temperature), whereas the intensity of the Soret band for $H_2TPP-NO_2$ is about half that for $H_2$-

**TABLE 1: Wavelengths (in nm[a]) of the Maxima of Electronic Absorption and Fluorescence Excitation Bands of $H_2TPP-NO_2$ in Different Solvents at Room and Liquid Nitrogen Temperatures**

| solvent/ temp | type of spectrum | B (Soret) | $Q_{Y01}$ | $Q_{Y00}$ | $Q_{X01}$ | $Q_{X00}$ |
|---|---|---|---|---|---|---|
| *n*-hexane/296 K | absorption | 421 | 522 | 555 | 600 | 657 |
| benzene/296 K | absorption | 429 | 526 | 560 | 604 | 664 |
| TDE[b]/296 K | absorption | 425 | 524 | 558 | 603 | 657 |
| TDE/77 K | absorption | 438 | 531 | 568 | 613 | 670 |
| TDE/77 K | fluor excitation ($\lambda_{reg} = 660$ nm) | 429 | 522 | 560 | 601 | 659[c] |
| TDE/77 K | fluor excitation ($\lambda_{reg} = 700$ nm) | 447 | 536 | 574 | 619 | 681 |

[a] ±1.0 nm. [b] Solvent mixture toluene/diethyl ether/ethanol (2:2:1). [c] This wavelength of the $Q_{X00}$ band maximum was evaluated empirically under the assumption that for the "blue-shifted" species the energy difference (in wavenumbers) between maxima of the $Q_{X00}$ and $Q_{X01}$ bands equals that measured for the "red-shifted" species.

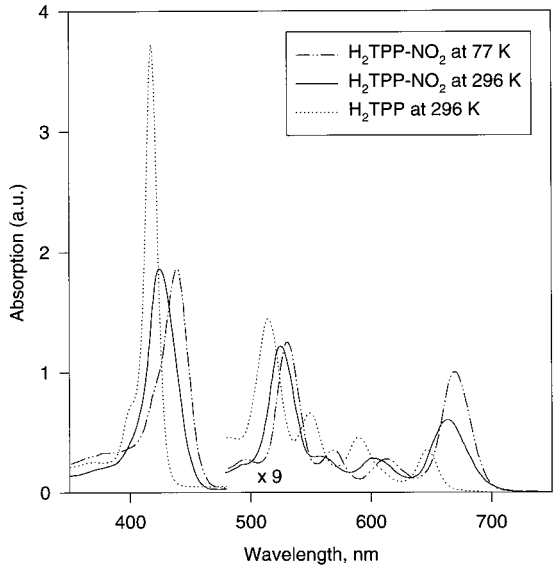


**Figure 2.** Absorption spectra of $H_2TPP-NO_2$ and $H_2TPP$ in the solvent mixture toluene/diethyl ether/ethanol (TDE, 2:2:1). The room-temperature spectra of $H_2TPP-NO_2$ and $H_2TPP$ were obtained at equal porphyrin concentrations. In the low-temperature spectrum of $H_2TPP-NO_2$, the Soret band intensity was normalized to that in the room-temperature spectrum.

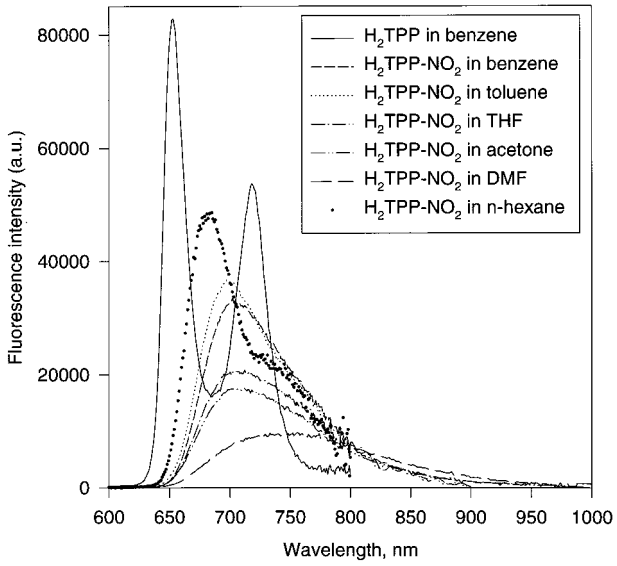


**Figure 3.** Fluorescence spectra of $H_2TPP-NO_2$ in different solvents and $H_2TPP$ in benzene. The spectra are matched to correspond to equal numbers of photons absorbed.

TPP at the same concentration (the extinction coefficient is not used here because that would not be valid for $H_2TPP-NO_2$ solutions; see below). The integral intensities of the Soret band are approximately equal for $H_2TPP-NO_2$ and $H_2TPP$. The width of the $Q_{X00}$ band for $H_2TPP-NO_2$ is also about twice that for $H_2TPP$ (840 and 480 $cm^{-1}$, respectively). Furthermore, a remarkably increased (integral) intensity of the $Q_{X00}$ band and a decreased intensity of the $Q_{Y00}$ band of $H_2TPP-NO_2$ as compared to those of $H_2TPP$ stand out. Although the general profile of the $H_2TPP-NO_2$ absorption spectrum remains the same in different solvents (Figure 2), the exact positions of the absorption band maxima clearly exhibit a dependence on the nature of the solvent (Table 1). Although this dependence is not very strong (the maximum shift is observed for the Soret band and equals ~8 nm for benzene with respect to that in *n*-hexane solution), it is markedly stronger than that observed for $H_2TPP$ (1−2 nm).

The main feature of the $H_2TPP-NO_2$ absorption spectrum at 77 K is a noticeable red shift of this spectrum as compared with the measured room-temperature absorption spectrum (Figure 2). This shift equals ~10 nm for the Soret band and ~6−10 nm for the Q bands (Table 1). Note also the increase of relative intensity of the $Q_{X00}$ band. In general, however, the low-temperature absorption bands remain as broad as those in the room-temperature spectrum.

**Fluorescence and Fluorescence Excitation Spectra.** In contrast to the absorption spectra, the room-temperature fluorescence spectra of $H_2TPP-NO_2$ show a strong dependence on the nature of the solvent (Figure 3). The main features of these fluorescence spectra are the following. First, the fluorescence peaks of these spectra are considerably red-shifted relative to the peaks of the corresponding longest wavelength absorption $Q_{X00}$ band; that is there is a large Stokes shift of the fluorescence. The magnitudes of the fluorescence Stokes shift/fluorescence maximum wavelength were found to be 420 $cm^{-1}$/683 nm in *n*-hexane, 810 $cm^{-1}$/702 nm in TDE, 900 $cm^{-1}$/706 nm in benzene, 1100 $cm^{-1}$/717 nm in acetone and tetrahydrofurane (THF), and 2040 $cm^{-1}$/768 nm in *N*,*N*-dimethyl-formamide (DMF). Clearly, the Stokes shift increases with an increase of the solvent polarity, using the microscopic empirical parameter $E_T^N$ to characterize the solvent polarity.[27] Second, in all solvents (except to some extent *n*-hexane), the fluorescence spectra of $H_2TPP-NO_2$ were found to be wide and structureless, in contrast to the structured bands usually observed for the tetraarylporphyrins. For example, $H_2TPP$ shows two narrow emission bands of similar intensity at 652 and 718 nm in benzene solution (Figure 3). Third, the fluorescence spectrum width also increases with an increase of the solvent polarity, and the most red-shifted and broad spectrum is observed for the most polar of the solvents, DMF. Finally, the fluorescence quantum yields, $\Phi_f$, of $H_2TPP-NO_2$ in all solvents were found to decrease with an increase of $E_T^N$ (Table 2). For the fluorescence quantum yield measurements, the fluorescence of $H_2TPP$ in air-saturated benzene solution was used as a reference with $\Phi_f = 0.09$.[28]

For all solvents at room temperature, no pronounced dependence was found of the fluorescence spectra on the excitation

**TABLE 2: Fluorescence Lifetimes, $\tau_1$, $\tau_2$, and Quantum Yields, $\Phi_f$, of $H_2TPP-NO_2$ and $H_2TPP$ in Different Solvents at Room Temperature**

| compound/ solvent | $E_T^N$ [a] | $\tau_1$[b,c], ns | $\tau_2$[b,c], ns | $\Phi_f$[d] $10^{-2}$ |
|---|---|---|---|---|
| $H_2TPP$/benzene | 0.111 | 9.4 | | 9.0[e] |
| $H_2TPP$/DMF[f] | 0.404 | 10.4 | | |
| $H_2TPP-NO_2$/*n*-hexane | 0.009 | 2.4 (0.6) | 4.1 (0.4) | 9.9 |
| $H_2TPP-NO_2$/toluene | 0.099 | 1.8 (0.3) | 3.1 (0.7) | 7.4 |
| $H_2TPP-NO_2$/benzene | 0.111 | 1.3 (0.6) | 2.7 (0.4) | 7.0 |
| $H_2TPP-NO_2$/acetone | 0.355 | 1.3 (0.6) | 2.1 (0.4) | 5.7 |
| $H_2TPP-NO_2$/DMF[f] | 0.404 | 0.9 | | 3.7 |

[a] Normalized empirical parameter of solvent polarity.[27] [b] Fluorescence lifetimes (time constants of the biexponential fitting); the numbers in parentheses are relative amplitudes of the two decay components. Standard errors ±0.1 ns. [c] The kinetic measurements were carried out at 688 (for *n*-hexane and TDE solutions) and 701 nm (for toluene, benzene, acetone, and DMF solutions). The excitation was at 505 nm in all cases. [d] The fluorescence quantum yield measured at 505 nm excitation. Reproducibility, ± 5%. [e] From ref 28. [f] *N*,*N*-dimethylformamide.

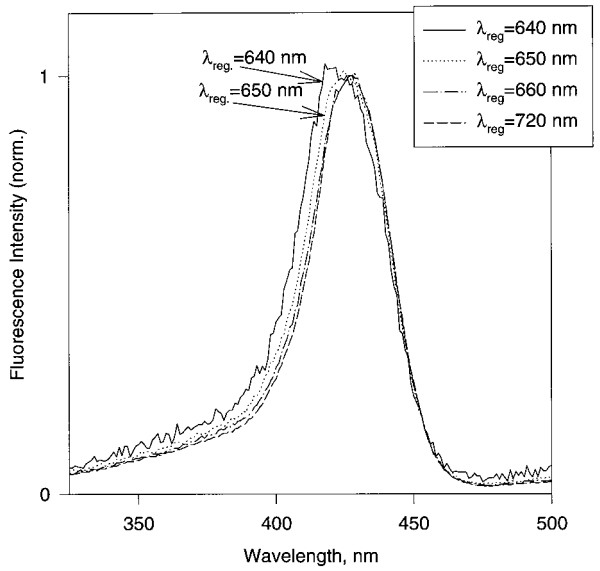


**Figure 4.** Fluorescence excitation spectra of $H_2TPP-NO_2$ in TDE at room temperature at different recording wavelengths (Soret band region).

wavelength and for the fluorescence excitation spectra on the recording wavelength. Only close inspection of the spectra shows that such dependence does indeed exist. For example, detection in the 660−750 nm spectral range results in quite identical fluorescence excitation spectra of $H_2TPP-NO_2$ in TDE at room temperature, and only detection at the blue side of the fluorescence spectrum (640−650 nm) reveals different, slightly blue-shifted fluorescence excitation spectra (Figure 4).

In contrast to the room-temperature results, the fluorescence spectra of $H_2TPP-NO_2$ in the TDE mixture measured at 77 K exhibit a strong dependence on the excitation wavelength. A careful analysis of many fluorescence and fluorescence excitation spectra, obtained at different excitation and detection wavelengths, respectively, has shown that two emitting species with slightly different absorption spectra are responsible for the 77 K $H_2TPP-NO_2$ fluorescence. The fluorescence spectra of these two species are similar but shifted with respect to each other (Figure 5) and consist of two well-resolved bands, like in the usual fluorescence spectra of "normal" porphyrins such as $H_2TPP$. The maxima of these two-band fluorescence spectra are found to be at 674/744 nm ("blue-shifted" species) and at 694/765 nm ("red-shifted" species). The fwhm values of the

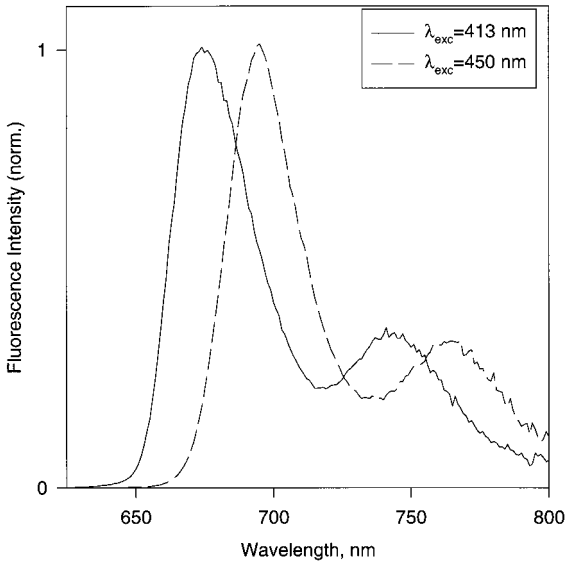


**Figure 5.** Fluorescence spectra of the blue-shifted ($\lambda_{exc}$ = 413 nm) and red-shifted species ($\lambda_{exc}$ = 450 nm) obtained in TDE at 77 K (see text).

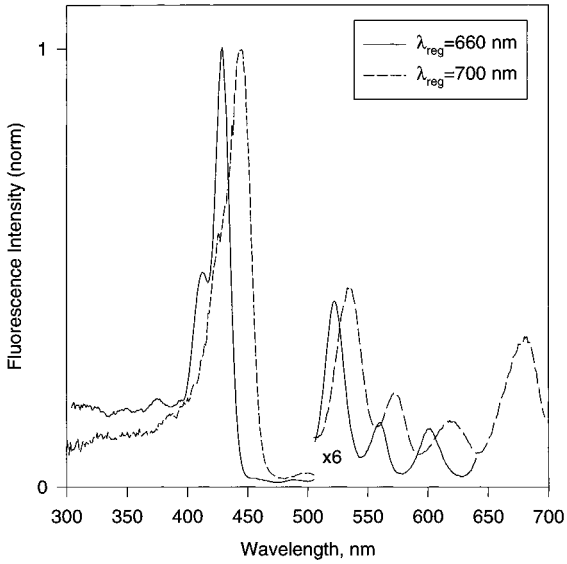


**Figure 6.** Fluorescence excitation spectra of the blue-shifted ($\lambda_{exc}$ = 660 nm) and red-shifted species ($\lambda_{exc}$ = 700 nm) obtained in TDE at 77 K (see text).

strongest (short-wavelength) bands are 780 and 660 $cm^{-1}$ for the blue-shifted and red-shifted species, respectively. Note that the fluorescence spectra, shown in Figure 5, were obtained at excitation conditions where only one of those species is preferentially excited. When arbitrary excitation wavelengths are used, the detected spectra are broader and more complex, due to emission from both species, and generally the fluorescence of the red-shifted species markedly prevails in such spectra.

Fluorescence excitation spectra of the two species at 77 K are shown in Figure 6. As with the fluorescence spectra, these spectra are similar but shifted in wavelength. The fluorescence excitation spectrum of the blue-shifted species exhibits a Soret band maximum at 429 nm (fwhm ∼900 $cm^{-1}$), whereas for the red-shifted species, the Soret band maximum is at 447 nm (fwhm ∼1800 $cm^{-1}$). The wavelengths of the Q band maxima for the fluorescence excitation spectra of both species are summarized in Table 1. It is interesting to note that at 77 K the fluorescence Stokes shifts for the blue-shifted and red-shifted

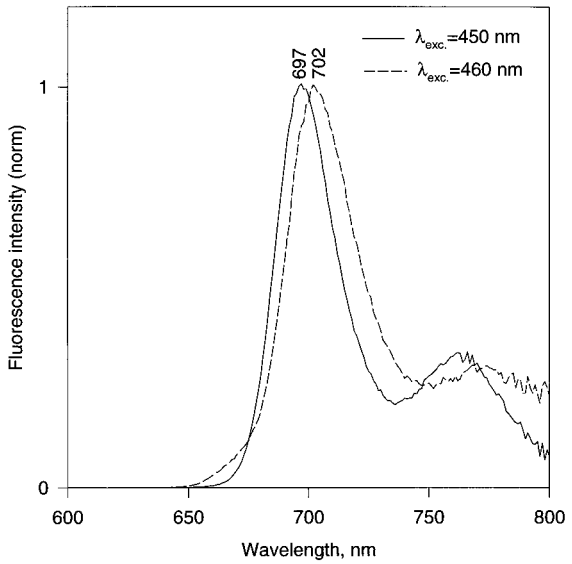


**Figure 7.** Dependence of the fluorescence spectra of $H_2TPP-NO_2$ (red-shifted species) in TDE at 77 K on the excitation wavelength. Numbers near peaks are wavelengths (in nm) of the corresponding fluorescence maxima.

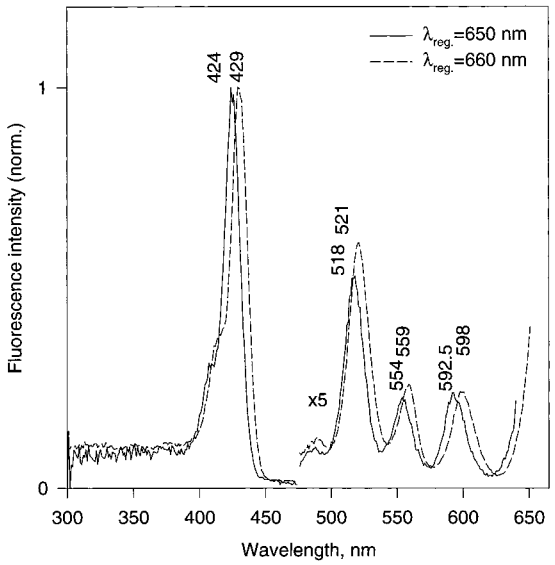


**Figure 8.** Dependence of the fluorescence excitation spectra of $H_2$-$TPP-NO_2$ (blue-shifted species) in TDE at 77 K on the recording wavelength. Numbers near peaks are wavelengths (in nm) of the corresponding maxima.

species are 340 and 275 $cm^{-1}$, respectively, considerably smaller than those at room temperature.

We note that the red shifted fluorescence excitation spectrum in Figure 6 shows broader bands as compared with the blue shifted spectrum, which is most likely related to the experimental difficulties to spectrally separate the red shifted excitation spectrum. It is not possible to record the fluorescence spectrum of the red-shifted species without some contribution of the fluorescence originating from the blue-shifted species (Figure 5). The opposite appears to be the case for the fluorescence spectra, where the blue-shifted fluorescence spectrum appears to be broader as compared to the red-shifted spectrum. Similarly to the fluorescence excitation spectra, this is most likely related to the overlap of the corresponding absorption spectra of the blue-shifted and red-shifted species (Figure 6). As a result, separate excitation is only possible for the red-shifted species but not for the blue-shifted one.

At 77 K, for each species, the exact position of the fluorescence spectrum was found to depend on the excitation wavelength, and a red shift of the excitation wavelength results in a corresponding red shift of the fluorescence spectrum. This shift has only an insignificant effect on the profile of the fluorescence spectrum (Figure 7, where this effect is shown for the blue-shifted species). In a similar manner, for each species, the exact position of the fluorescence excitation spectrum depends on the recording wavelength, and a red shift of the recording wavelength results in a corresponding red shift of the fluorescence excitation spectrum, without any significant change in its profile. Figure 8 shows this effect for the red-shifted species. These observations are evidence of a large spectral inhomogeneity of both $H_2TPP-NO_2$ species at 77 K. Reference experiments with $H_2TPP$ have shown that, under the same conditions, spectral shifts of the fluorescence and fluorescence excitation spectra for this molecule do not exceed 1−2 nm.

Finally, it is found that at 77 K a small but detectable mutual phototransformation occurs between the blue-shifted and red-shifted species. This results in small changes of the fluorescence and fluorescence excitation spectra after each spectrum is recorded, and these changes accumulate with each new spectral recording. These changes are, however, fully reversible by thawing and freezing the solutions. All spectra shown in Figures 5−8 were obtained with freshly frozen solutions, which were kept from illumination before the recording the spectrum.

**Fluorescence Kinetics.** The room-temperature fluorescence kinetics of $H_2TPP-NO_2$ reveal several peculiarities as compared to that of $H_2TPP$. First, the lifetimes are considerably shorter than those of the $H_2TPP$. For $H_2TPP-NO_2$, the longest lifetimes are found for low-polarity solvents and are in the range of 2−4 ns (Table 2), whereas for $H_2TPP$, lifetimes of 9.5−10.5 ns were found in all solvents listed in Table 2, independent of their polarity. The latter values are in good agreement with literature data of $H_2TPP$ fluorescence lifetimes for air-saturated methanol (10.6 ns[29]) and propanol (9.4 ns[30]) as solvents. Second, the fluorescence kinetics could not be fitted with a single-exponential decay for any of the used solvents. Within the experimental accuracy, the data can be satisfactorily fitted to a biexponential fluorescence decay $I(t) = A_1 \exp(-t/\tau_1) + A_2 \exp(-t/\tau_2)$. Finally, the fluorescence decay kinetics were found to be dependent on the polarity of the applied solvent, and the shortest lifetime (0.9 ns) was found in the most polar solvent, DMF. The corresponding time constants $\tau_1$ and $\tau_2$ and their relative amplitudes $A_1$ and $A_2$ (in parentheses) obtained for different solvents are summarized in Table 2. The relative amplitudes $A_1$ and $A_2$ were of comparable magnitudes in all solvents and at all recording wavelengths.

**Picosecond Transient Absorption Spectra.** Transient absorption (TA) spectra were measured for $H_2TPP-NO_2$ in benzene and DMF solutions. These TA spectra were found to be qualitatively similar, and Figure 9 shows, as an example, the TA spectra for a DMF solution at different time delays between the pump and probe pulses. The maximum value of the absorption changes following excitation is found at ∼50 ps delay. This value correlates well with the pulse duration (25 ps fwhm) and the fairly long lifetime of the first excited species (see below). The 50 ps spectrum shows a positive sign of $\Delta A$ (i.e., an increase of absorption) over the 460−780 nm spectral range. Nevertheless, the ground-state absorption bands are seen in this spectrum as dips at 525 nm ($Q_{Y01}$), 560 nm ($Q_{Y00}$), 605 nm ($Q_{X01}$), and 665 nm ($Q_{X00}$). A characteristic stimulated emission feature is also observed as a trough in the 690−800 nm region, with a minimum near 750−760 nm. Stimulated emission is characteristic for porphyrin $^1(\pi,\pi^*)$ states.[31] The

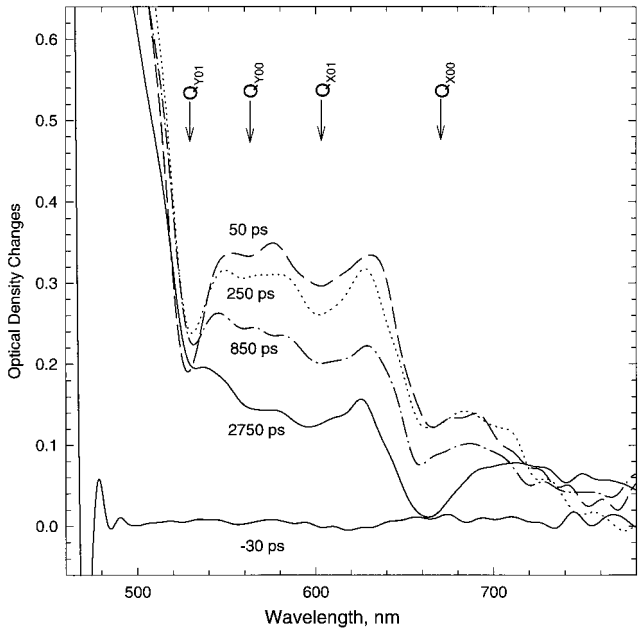


**Figure 9.** Absorption difference spectra of $H_2TPP-NO_2$ in DMF at 296 K at different delay times (indicated as numbers near curves). Arrows indicate positions of the corresponding ground-state absorption maxima.

50 ps spectrum decays with an ~1 ns time constant, and a new TA spectrum is completed at 2.75 ns delay and does not change anymore on a 10 ns time scale. The second TA spectrum is generally similar to the first (50 ps delay) TA spectrum, except (1) the absence of a trough in the 690−800 nm region and (2) approximately a 2 times smaller $\Delta A$ value in the region 550−650 nm, where the ground-state absorption is small. These features are in agreement with the triplet $^3(\pi,\pi^*)$ origin of the second (long-lived) excited state.[31] The triplet quantum yield $\Phi_T$ may be estimated to be ~0.4 in DMF and ~0.65 in toluene (not shown), because extinctions of the $S_1 \rightarrow S_n$ and $T_1 \rightarrow T_n$ absorptions are usually very close for the porphyrins in the spectral region between the Soret band and the $Q_{X00}$ band.[31] This is in good agreement with the value $\Phi_T = 0.62$ obtained for the related compound 2-nitrotetra-*p*-tolylporphyrin in benzene.[7]

**Quantum Chemical Calculations.** Tables 3 and 4 summarize the results of the ZINDO/S calculations performed for the C and O tautomers, respectively, as a function of the dihedral angle $\theta$ between the $NO_2$ and porphyrin planes, yielding the positions of the $S_0 \rightarrow S_n$ transitions, their oscillator strengths, and the dipole moments of the molecules in the ground and excited state. Additionally, for the lowest excited singlet state, $S_1$, the fractional charge $q$ (in percent) that is transferred from the porphyrin ring to the $NO_2$ group is calculated. The initial geometry was taken to have $\theta = 80°$, resulting from the geometry optimization using the PM3 method. For simplicity, $NO_2$ rotation was considered only to the side of smaller $\theta$ values as compared to the equilibrium $\theta = 80°$. The calculations for $\theta < 80°$ were carried out with the remainder of the porphyrin structure being identical to the optimized one. A graphical presentation of the most important results of these calculations is given in Figures 10 and 11.

Although the calculated energies of the lowest excited $Q_{X00}$ and $Q_{Y00}$ states ($S_0 \rightarrow S_1$ and $S_0 \rightarrow S_2$ transitions for the optimized geometry) are evidently lower than the experimental values and the calculated energies of the B states ($S_0 \rightarrow S_5$ and $S_0 \rightarrow S_6$ transitions for the optimized geometry) are evidently higher than the experimental values which is common for

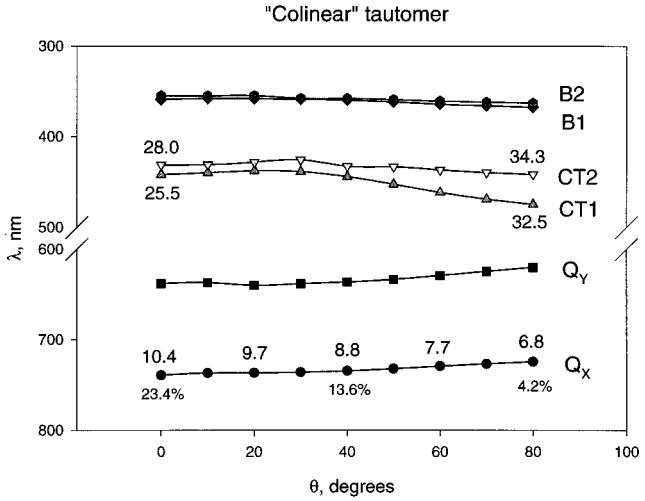


**Figure 10.** Scheme of the energy levels of $H_2TPP-NO_2$ ("collinear" tautomer) calculated by ZINDO/S as a function of the angle $\theta$ between the $NO_2$ and porphyrin planes. The numbers are calculated dipole moments (in Debye units), and the numbers in percents are the calculated fractional charges transferred from the porphyrin ring to $NO_2$ group.

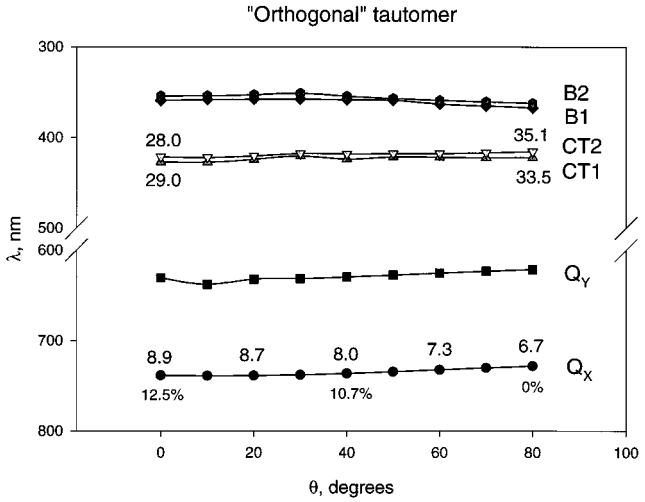


**Figure 11.** Energy level scheme of $H_2TPP-NO_2$ ("orthogonal" tautomer). See the caption of Figure 10 for details.

semiempirical calculations of tetrapyrrolic compounds,[32] more important is that (1) the energy level scheme of $H_2TPP-NO_2$ can be successfully described in the usual terms of porphyrinic $Q_X$, $Q_Y$, and B states plus two new charge transfer (CT) states and (2) the calculations predict changes of the energy level scheme as a function of the dihedral angle $\theta$ between the $NO_2$ group plane and the porphyrin plane.

Note, first of all, the regularities that are common for both tautomers. (1) The energies of the $Q_X$, $Q_Y$, and B states decrease with a decrease of $\theta$. On the other hand, the energies of the B states increase with a decrease of $\theta$.

(2) The dipole moment $\mu_1$ of the lowest excited singlet state $Q_X$ increases with a decrease of $\theta$.

(3) The ground-state dipole moment $\mu_0$ also increases with a decrease of $\theta$, but this increase is less than that for the lowest excited state, and the difference $\mu_1 - \mu_0$ increases with a decrease of $\theta$.

(4) For $\theta < 50°$, new transitions arise that do not belong to the transitions between the four "standard" porphyrin orbitals[33] and are formed by the one-electron excitations from the orbital localized on the phenyl ring nearest to the $NO_2$ group.

**TABLE 3: Calculated Dependencies for Tautomer C of the Positions of the Singlet−Singlet Transitions ($\lambda$), Dipole Moment ($\mu$); Oscillator Strength ($f$), and the Fractional Charge ($q$) Transferred from the Porphyrin Ring to the $NO_2$ Group, upon the Angle $\theta$ between the $NO_2$ Group and the Plane of the Porphyrin[a]**

| | angle, degree | | | | | | | | |
|---|---|---|---|---|---|---|---|---|---|
| | 0 | 10 | 20 | 30 | 40 | 50 | 60 | 70 | 80 |
| | | | | $S_0$ | | | | | |
| $\mu$, Debye | 8.708 | 8.722 | 8.556 | 8.267 | 7.939 | 7.588 | 7.276 | 7.022 | 6.820 |
| | | | | $S_0 \rightarrow S_1$ | | | | | |
| $\lambda$, nm | *739.4* | *736.9* | *736.8* | *736.0* | *734.6* | *732.1* | *729.4* | *726.8* | *724.5* |
| $f$ | *0.010* | *0.013* | *0.013* | *0.011* | *0.009* | *0.007* | *0.006* | *0.005* | *0.005* |
| $\mu$, Debye | *10.439* | *9.985* | *9.712* | *9.245* | *8.755* | *8.193* | *7.659* | *7.185* | *6.786* |
| q, % | *23.4* | *14.4* | *14.1* | *13.5* | *13.6* | *13.7* | *13.5* | *11.7* | *4.2* |
| | | | | $S_0 \rightarrow S_2$ | | | | | |
| $\lambda$, nm | 730.5 | 670.1 | *639.7* | *637.9* | *636.1* | *633.1* | *628.9* | *624.3* | *619.9* |
| $f$ | 0.012 | 0.010 | *0.074* | *0.070* | *0.064* | *0.056* | *0.048* | *0.041* | *0.036* |
| $\mu$, Debye | 10.281 | 13.375 | *10.735* | *10.411* | *10.017* | *9.477* | *8.821* | *8.044* | *7.212* |
| | | | | $S_0 \rightarrow S_3$ | | | | | |
| $\lambda$, nm | *637.7* | *636.8* | 557.7 | 471.4 | ***444.2*** | ***452.5*** | ***461.5*** | ***469.0*** | ***474.7*** |
| $f$ | *0.078* | *0.078* | 0.012 | 0.008 | ***0.581*** | ***0.412*** | ***0.247*** | ***0.115*** | ***0.015*** |
| $\mu$, Debye | *10.965* | *10.861* | 13.735 | 13.315 | ***27.582*** | ***28.582*** | ***29.871*** | ***31.209*** | ***32.529*** |
| | | | | $S_0 \rightarrow S_4$ | | | | | |
| $\lambda$, nm | ***442.0*** | ***439.9*** | ***437.8*** | ***438.7*** | ***432.8*** | ***433.5*** | ***436.9*** | ***439.7*** | ***441.8*** |
| $f$ | ***0.541*** | ***0.595*** | ***0.669*** | ***0.676*** | ***0.298*** | ***0.251*** | ***0.150*** | ***0.070*** | ***0.009*** |
| $\mu$, Debye | ***25.525*** | ***26.926*** | ***26.926*** | ***26.936*** | ***25.908*** | ***30.595*** | ***32.214*** | ***33.393*** | ***34.291*** |
| | | | | $S_0 \rightarrow S_5$ | | | | | |
| $\lambda$, nm | ***431.5*** | ***431.0*** | ***428.4*** | ***425.7*** | 409.3 | 377.4 | **364.1** | **365.8** | **367.3** |
| $f$ | ***0.621*** | ***0.694*** | ***0.633*** | ***0.505*** | 0.052 | 0.045 | **3.062** | **3.195** | **3.277** |
| $\mu$, Debye | ***28.062*** | ***28.365*** | ***28.235*** | ***27.725*** | 14.065 | 13.980 | **8.472** | **7.890** | **7.526** |
| | | | | $S_0 \rightarrow S_6$ | | | | | |
| $\lambda$, nm | 415.7 | 403.8 | 378.4 | **358.6** | **359.5** | **361.5** | **360.6** | **361.7** | **362.7** |
| $f$ | 0.201 | 0.087 | 0.125 | **1.980** | **2.742** | **2.832** | **2.985** | **3.148** | **3.215** |
| $\mu$, Debye | 12.039 | 13.305 | 12.627 | **7.101** | **9.102** | **8.438** | **7.620** | **7.431** | **7.164** |
| | | | | $S_0 \rightarrow S_7$ | | | | | |
| $\lambda$, nm | 377.7 | 368.3 | **357.9** | **357.6** | **357.7** | **359.0** | | | |
| $f$ | 0.071 | 0.120 | **2.651** | **2.832** | **2.775** | **2.939** | | | |
| $\mu$, Debye | 17.090 | 16.686 | **8.955** | **8.115** | **8.544** | **8.243** | | | |
| | | | | $S_0 \rightarrow S_8$ | | | | | |
| $\lambda$, nm | **358.8** | **357.7** | **354.6** | | | | | | |
| $f$ | **1.961** | **2.309** | **2.290** | | | | | | |
| $\mu$, Debye | **9.291** | **8.876** | **9.031** | | | | | | |
| | | | | $S_0 \rightarrow S_9$ | | | | | |
| $\lambda$, nm | **354.7** | **354.8** | | | | | | | |
| $f$ | **2.440** | **2.388** | | | | | | | |
| $\mu$, Debye | **9.446** | **9.458** | | | | | | | |

[a] The numbers marked by the italic or bold fonts indicate one-electron transitions between the four "standard" porphyrin orbitals; these transitions are full analogs of the usual porphyrinic Q and B states, respectively. The numbers marked by the bold italic font correspond to transitions from the porphyrin orbitals to the orbital localized on the $NO_2$ group (CT transitions). Other transitions are formed by one-electron excitations from the orbital that is localized on the phenyl ring nearest to the $NO_2$ group.

There are differences between the two tautomers. (1) The energy of the $Q_X$ state is slightly lower for the O tautomer. (2) The energies of the two CT states are lower for the C tautomer. With a decrease of $\theta$, the energies of the CT states increase for the C tautomer and are almost unaffected for the O tautomer.

## Discussion

**Absorption Spectra.** As is shown by NMR measurements, $H_2TPP-NO_2$ exists in solutions as an equilibrium mixture of the two tautomers, O and C[11,12] (Figure 1). It is also found[11] that the tautomer O is the more stable one, and at 200 K in $CD_2Cl_2$ solution its fractional population $P_O(200) = 0.97$, where $P_O = [O]/([O] + [C])$ and [O] and [C] are the tautomer O and C concentrations, respectively. Furthermore, if two tautomeric species, O and C, are in equilibrium and C is less stable than O by $\Delta E$ (neglecting entropy changes), then the fractional population of O as a function of temperature, $P_O(T)$, is simply given by the expression

$$P_O(T) = [1 + \exp(-\Delta E/kT)]^{-1} \quad (1)$$

It follows from the eq 1 and the $P_O(200)$ value that $\Delta E \approx 180\ cm^{-1}$. Using this $\Delta E$ value, the room-temperature fractional population of the tautomer O can be easily found; $P_O(296) = 0.70$. (Note that this value of $P_O(296)$ is exact only for $CD_2Cl_2$ solution and may depend on the solvent used[11]).

The above reasoning leads to a reasonable explanation for the changes of the $H_2TPP-NO_2$ absorption spectrum with temperature (Figure 2), as a result of changes of the fractional populations $P_O$ and $P_C$. This results in the following conclusions. (i) The tautomer O absorption spectrum is red-shifted with respect to that of tautomer C. This is generally consistent with the predictions of the quantum chemical calculations. (ii) The intensity of the $Q_{X00}$ absorption band (relative to the intensities of the other Q bands) is higher for the tautomer O than for the tautomer C. Quantum chemical calculations predict, however, opposite behavior and therefore are in contradiction

**TABLE 4: Calculated Dependencies for Tautomer O of the Positions of the Singlet−Singlet Transitions (λ), Dipole Moment (μ); Oscillator Strength (*f*), and the Fractional Charge (*q*) Transferred from the Porphyrin Ring to $NO_2$ Group, upon the Angle θ between the $NO_2$ Group and the Plane of the Porphyrin[a]**

| | angle, degrees | | | | | | | | |
|---|---|---|---|---|---|---|---|---|---|
| | 0 | 10 | 20 | 30 | 40 | 50 | 60 | 70 | 80 |
| | | | | $S_0$ | | | | | |
| μ, Debye | 8.007 | 7.987 | 7.851 | 7.671 | 7.405 | 7.150 | 6.940 | 6.777 | 6.634 |
| | | | | $S_0 \rightarrow S_1$ | | | | | |
| λ, nm | *738.9* | *739.2* | *739.0* | *738.1* | *736.7* | *734.7* | *732.5* | *730.4* | *728.3* |
| *f* | *0.006* | *0.005* | *0.004* | *0.004* | *0.003* | *0.002* | *0.001* | *0.001* | *0.001* |
| μ, Debye | *8.851* | *8.850* | *8.657* | *8.421* | *8.019* | *7.626* | *7.279* | *6.992* | *6.729* |
| *q*, % | *12.5* | *12.7* | *12.2* | *11.6* | *10.7* | *9.7* | *7.9* | *4.9* | *0.0* |
| | | | | $S_0 \rightarrow S_2$ | | | | | |
| λ, nm | 674.1 | *637.7* | *632.1* | *631.4* | *629.6* | *627.5* | *625.3* | *623.2* | *621.3* |
| *f* | 0.001 | *0.000* | *0.001* | *0.001* | *0.000* | *0.000* | *0.000* | *0.001* | *0.002* |
| μ, Debye | 14.461 | *10.636* | *9.667* | *9.423* | *8.943* | *8.453* | *7.998* | *7.601* | *7.225* |
| | | | | $S_0 \rightarrow S_3$ | | | | | |
| λ, nm | *630.5* | 625.4 | 542.5 | 460.6 | ***423.8*** | ***421.4*** | ***421.8*** | ***422.1*** | ***422.0*** |
| *f* | *0.002* | 0.003 | 0.004 | 0.011 | ***0.430*** | ***0.493*** | ***0.385*** | ***0.210*** | ***0.011*** |
| μ, Debye | *9.828* | 10.162 | 13.973 | 13.547 | ***25.322*** | ***28.826*** | ***30.391*** | ***31.942*** | ***33.547*** |
| | | | | $S_0 \rightarrow S_4$ | | | | | |
| λ, nm | ***427.2*** | ***427.4*** | ***424.3*** | ***420.6*** | ***418.1*** | ***417.9*** | ***417.7*** | ***416.8*** | ***415.5*** |
| *f* | ***0.301*** | ***0.313*** | ***0.333*** | ***0.344*** | ***0.541*** | ***0.341*** | ***0.184*** | ***0.092*** | ***0.005*** |
| μ, Debye | ***28.984*** | ***29.672*** | ***29.725*** | ***30.113*** | ***30.321*** | ***31.597*** | ***32.839*** | ***33.931*** | ***35.108*** |
| | | | | $S_0 \rightarrow S_5$ | | | | | |
| λ, nm | ***421.6*** | ***422.2*** | ***420.5*** | 417.9 | 397.1 | 365.3 | **362.6** | **364.6** | **366.7** |
| *f* | ***0.939*** | ***0.929*** | ***0.913*** | 0.831 | 0.068 | 0.675 | **2.983** | **3.111** | **3.269** |
| μ, Debye | ***27.984*** | ***27.804*** | ***27.671*** | 26.537 | 13.602 | 10.970 | **9.328** | **8.757** | **7.801** |
| | | | | $S_0 \rightarrow S_6$ | | | | | |
| λ, nm | 416.1 | 405.5 | 381.8 | **357.3** | **357.9** | **358.5** | **358.5** | **360.1** | **361.7** |
| *f* | 0.036 | 0.024 | 0.044 | **2.955** | **2.938** | **2.336** | **3.161** | **3.284** | **3.389** |
| μ, Debye | 12.249 | 12.493 | 12.155 | **8.905** | **9.028** | **8.110** | **8.760** | **8.310** | **7.813** |
| | | | | $S_0 \rightarrow S_7$ | | | | | |
| λ, nm | 380.6 | 372.3 | **357.5** | **355.7** | **354.0** | **356.5** | | | |
| *f* | 0.015 | 0.025 | **2.710** | **1.346** | **2.849** | **2.922** | | | |
| μ, Debye | 19.584 | 19.449 | **7.957** | **3.938** | **9.604** | **9.173** | | | |
| | | | | $S_0 \rightarrow S_8$ | | | | | |
| λ, nm | **358.8** | **358.0** | **354.0** | **350.9** | | | | | |
| *f* | **2.386** | **2.611** | **1.065** | **1.498** | | | | | |
| μ, Debye | **9.802** | **9.399** | **8.779** | **4.557** | | | | | |
| | | | | $S_0 \rightarrow S_9$ | | | | | |
| λ, nm | **353.9** | **353.6** | **352.5** | | | | | | |
| *f* | **2.601** | **2.646** | **1.809** | | | | | | |
| μ, Debye | **9.779** | **9.779** | **3.927** | | | | | | |

[a] The numbers marked by the italic or bold fonts indicate one-electron transitions between the four "standard" porphyrin orbitals; these transitions are full analogs of the usual porphyrinic Q and B states, respectively. The numbers marked by the bold italic font correspond to transitions from the porphyrin orbitals to the orbital localized on the $NO_2$ group (CT transitions). Other transitions are formed by one-electron excitations from the orbital that is localized on the phenyl ring nearest to the $NO_2$ group.

with the experimental results. The reason for this is not yet clear, but most likely a parametrization of the ZINDO/S method is not sufficiently accurate to predict such details for the spectra of the tautomers C and O. (iii) The large widths of $H_2TPP-NO_2$ absorption bands, found both at room and liquid nitrogen temperatures, cannot be explained only by the overlap of absorption spectra of two tautomeric forms. Indeed, in agreement with eq 1, at 77 K the absorption spectrum should belong mainly to the tautomer O. Since this spectrum remains broad, this implies that a large inhomogeneous broadening exists even at 77 K and this broadening is a characteristic of each of the two tautomers (see below).

The unusual dependence of the $H_2TPP-NO_2$ absorption spectrum on the nature of the solvent (Table 1) can now be explained by small variations of $P_O$ and $P_C$ fractions with a change of solvent. Small changes of $P_O$ and $P_C$ in various solvents were previously observed for $H_2TPP-NO_2$ at 200 K using NMR.[11]

**Fluorescence and Fluorescence Excitation Spectra.** We now discuss the 77 K $H_2TPP-NO_2$ fluorescence and fluorescence excitation spectra (Figures 5−8). Clearly, the blue-shifted and red-shifted species observed by their 77 K fluorescence and fluorescence excitation spectra are the tautomers C and O, respectively. The predominance of the red-shifted fluorescence in $H_2TPP-NO_2$ low-temperature fluorescence spectra found for the majority of arbitrary excitation wavelengths is consistent with the tautomer O predominance at lowered temperatures.[11] Note also that at 77 K these tautomers should be mutually independent, i.e., the tautomeric exchange, involving inner hydrogen migration, should be frozen. The rate constant for tautomeric exchange strongly depends on temperature. For example, for the related β-monosubstituted porphyrins at 196 K this rate constant ($k_{CO}$ in Figure 12) is about 20 $s^{-1}$.[12] When the activation energy of ∼4000 $cm^{-1}$ [12] for the tautomeric exchange for the β-monosubstituted porphyrins is considered, this exchange should be fully frozen at 77 K.

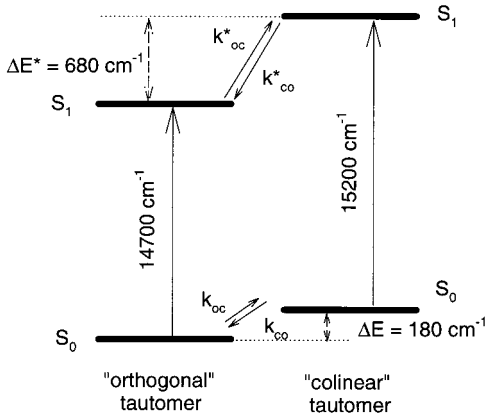


**Figure 12.** Energy levels of the "orthogonal" and "collinear" tautomers of $H_2TPP-NO_2$. Only the ground and lowest excited singlet states are shown. The scheme is valid for rigid glass solutions at 77 K, when conformational relaxation is frozen (see text).

Figure 12 represents the energy diagram of the ground ($S_0$) and lowest excited singlet ($S_1$) levels of the O and C tautomers. It has been assumed that the energies, $E(S_1)$, of the tautomers are equal to the wavenumbers of the maxima of the 77 K $Q_{X00}$ fluorescence excitation bands, yielding $E(S_1) = 14\,700$ cm$^{-1}$ for the tautomer O (red-shifted species) and $E(S_1) = 15\,200$ cm$^{-1}$ for the tautomer C (blue-shifted species). Since $\Delta E = 180$ cm$^{-1}$, this results in $\Delta E^* = 680$ cm$^{-1}$. The $E(S_1)$ energies, shown in this diagram, should rather be considered as averaged values, taking into account the dependence of the fluorescence spectra on the excitation wavelength and the fluorescence excitation spectra on the recording wavelength found at 77 K for each of the tautomers.

The spectral properties of the individual tautomers are remarkable. First of all, the fluorescence Stokes shifts observed for the individual tautomers at 77 K are as small as $\sim$300 cm$^{-1}$. A comparison with the Stokes shifts found for the room-temperature solutions suggests that different mechanisms must be responsible for the low-temperature and room-temperature Stokes shifts. We note that $H_2TPP-NO_2$ is a polar molecule, and its static dipole moment in the ground state is found to be 6.7 D at equilibrium geometry by semiempirical calculations (Tables 3 and 4). Excitation to the $S_1$ state results in a further increase of the dipole moment, and a reorientation of the solvent molecules around $H_2TPP-NO_2$ in the $S_1$ state should result in further stabilization, that is to a Stokes shift of the fluorescence spectrum relative to its initial position immediately after excitation (see below). Such solvent induced stabilization of the $S_1$ state is eliminated in a rigid glass at 77 K. The small Stokes shift, which is still observed at 77 K, is most likely explained by small changes of the porphyrin in-plane geometry after excitation. Participation of the $NO_2$ group rotation as a coordinate of the $S_1$ state stabilization at 77 K is less probable, because this rotation is strongly restricted at 77 K due to the solvent rigidity, and, besides, there is no pronounced driving force for such a rotation at 77 K, contrary to the conditions at room temperature (see below).

As shown in Figures 7 and 8, the spectra of both tautomers at 77 K exhibit a remarkable inhomogeneous broadening, which manifests itself as a dependence of the fluorescence spectral position on the excitation wavelength and of the fluorescence excitation spectral position on the recording wavelength. This inhomogeneity is most likely responsible for the large widths of the $H_2TPP-NO_2$ absorption bands and may have two main reasons: (1) different dispositions of the solvent molecules around the polar solute molecules and (2) different values of the angle between the $NO_2$ group plane and the plane of the porphyrin in the ground state.

Our quantum chemical calculations indicate the importance of the second mechanism. Indeed, the calculations predict that the energy of the $Q_X$ state should depend on $\theta$. On the other hand, the Boltzmann distribution of the $S_0$ state population around the optimized $\theta$ value cannot be very broad at 77 K, because our calculations predict the energy barrier for the $NO_2$ group rotation between $\theta = 80°$ and $\theta = 0°$ to be $\sim$4000 cm$^{-1}$. However, there may be two reasons for a much broader distribution than that predicted by the calculations made at "in a vacuum" conditions. First, the fast freezing of the solutions from 296 K (liquid solution) to 77 K (rigid glass solution), used in our experiments, can result in a $\theta$ distribution which is characteristic for higher temperatures. Second, the initial room temperature $\theta$ distribution can be much broader in polar solvents than that predicted by the calculations, because the stabilizing interaction of the polar $H_2TPP-NO_2$ molecule with polar solvent should decrease the barrier between the 80° and 0° conformations. Indeed, the ground-state dipole moment increases with a decrease of $\theta$, and therefore the stabilization effect should be larger for the molecules with smaller $\theta$ values. Note also that an excitation wavelength dependence of the fluorescence in rigid media at 77 K is frequently observed for flexible polar molecules (see, for example, refs 34 and 35).

In contrast to the conditions at low temperature, room-temperature fluorescence spectra of $H_2TPP-NO_2$ do not show pronounced spectral evidence for the existence of two different tautomers in solution. Indeed, only very careful spectral measurements show that there is a small dependence of the fluorescence spectra on the excitation wavelength (not shown) and, consequently, a dependence of the fluorescence excitation spectra on the recording wavelength (Figure 4). We suggest that the blue shift of the fluorescence excitation spectrum shown in Figure 4, detected at 640−650 nm, is a result of the preferential detection of the C (blue-shifted) tautomer. Since the differences between the O and C tautomer fluorescence spectra at room temperature are quite small, the interactions of the excited porphyrin with solvent molecules are relatively strong at room temperature, and these interactions result in almost identical and strongly inhomogeneously broadened fluorescence spectra of both tautomers.

Note that inner hydrogen migration in the porphyrin fluorescent state could in principle also result in the observed equivalence of the fluorescence spectra of the tautomers. Then, the exchange rate constant should be comparable to or higher than the fluorescence decay rate constant, which is of the order of $\sim 10^9$ s$^{-1}$. To the best of our knowledge, the tautomeric exchange rates are not known for the porphyrins in the excited state. A value of $\sim$104 s$^{-1}$ was found for the $\beta$-substituted porphyrins in the ground state at 292 K,[12] and most likely a value of the same order applies to the tautomeric exchange rate constant for the $S_1$ state of $\beta$-substituted porphyrins. To some extent, this is supported by literature data,[36−38] where different fluorescence spectra were found for two NH tautomers at room temperature for a series of asymmetrically substituted free base porphyrins, including the $\beta$-tetra-substituted compound 2,3,12,-13-tetraethylporphyrin. The observed biexponential fluorescence decay in all the solvents used (except DMF) may be also considered as evidence for the coexistence of two tautomers of $H_2TPP-NO_2$ that are not in equilibrium on the time scale of the fluorescence lifetimes (see below).

The origin of the broad and red-shifted fluorescence spectra, observed in the majority of the solvents used at room temper-

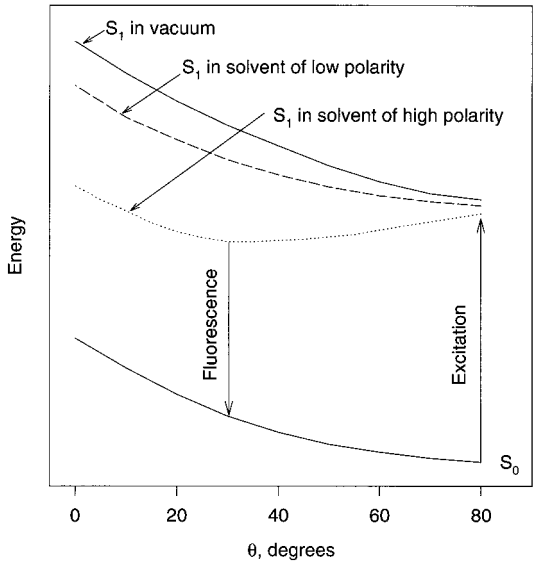


**Figure 13.** Schematic potential energy diagram for the ground $S_0$ and excited $S_1$ states of $H_2TPP-NO_2$. The ordinate represents energy, and the abscissa represents the angle $\theta$ between the $NO_2$ and porphyrin planes. Solid lines represent the situation in a vacuum. The dashed and dotted lines represent the situation in low-polarity and high-polarity solvents, respectively.

ature, can be qualitatively understood on the basis of our quantum chemical calculations (Tables 3 and 4 and Figures 10 and 11). A decrease of the $Q_X$ state energy with a decrease of $\theta$, as well as an increase of the $Q_X$ state dipole moment and, consequently, an increase of the solvent-induced stabilization effect with a decrease of $\theta$ should result in flattening of the $Q_X$ state energy vs $\theta$ curve, most likely resulting in formation of a minimum at $\theta < 80°$ (Figure 13). This should evidently result in a broadening and red shift of the fluorescence spectrum. Since for *n*-hexane, which is a very low-polarity solvent, such a solvent-induced flattening of the $E_Q(\theta)$ curve should be small, the fluorescence spectrum in this case should be much more narrow and close to the "normal" porphyrinic fluorescence spectra. As it is seen from the Figure 3 that this is indeed experimentally observed.

**Fluorescence Kinetics.** The experimental fluorescence decay kinetics clearly indicate the presence of two emitting species, which can be reasonably related to the two tautomers. (Note that biexponential fluorescence kinetics for some β-nitro-substituted free base porphyrins was also reported in ref 10 and attributed to "either different emitting species or a broad angular distribution of the emitting state".[10]) The question is, which tautomer exhibits the longer and which one the shorter fluorescence lifetime and what the reasons are for the difference. Our semiempirical calculations show that there is indeed a physical reason for the different fluorescence lifetimes for the different tautomers, i.e., a different energy of the CT states for the two tautomers. For both tautomers, the CT states are much higher in energy (in a vacuum) than the fluorescent $Q_X$ state. However, for the tautomer C, the CT state energy is ~2500 $cm^{-1}$ closer to that of the fluorescent $Q_X$ state than for the tautomer O. Since these CT states have a large dipole moment (~33−35 D for both tautomers at the equilibrium geometry), they should considerably decrease their energies in the solvents of high and probably even moderate polarity. We suggest that in polar solvents the CT states are so close to the fluorescent $Q_X$ state (remaining still higher in energy) that they can be (1) thermally populated from the $Q_X$ state and/or (2) quantum mechanically mixed with the $Q_X$ state.

The experimental data, in particular the temperature dependencies, do not allow one to distinguish between these two alternative mechanisms of the CT and $Q_X$ states interaction in polar solvents. In any case, the participation of CT states in the formation of the fluorescence state corresponds in fact to the participation of the (resonance) electronic structure with full electron transfer from the porphyrin ring to the $NO_2$ group. As a result of the short distance between the oxidized and reduced subunits, fast charge recombination should result in a very short lifetime of the CT (resonance) structure (see also Introduction). Therefore, the participation of the full CT structures in formation of the fluorescent $Q_X$ state should result in quenching of the latter. We believe that this quenching effect should be more effective for the C tautomer because of its lower lying CT state. On the basis of this reasoning, the shorter lifetimes in Table 2 are ascribed to the tautomer C, whereas the longer lifetimes are ascribed to the tautomer O. In DMF (the most polar solvent of the used), the two tautomers probably exhibit equally short fluorescence lifetimes (0.9 ns). (Note that the values $A_1$ and $A_2$ in Table 2 cannot be used as indicators of the C and O tautomers, fractional populations, because the $A_1/A_2$ ratio is determined not only by the fractional population ratio $P_C/P_O$ but also by the (unknown) ratio of the photon numbers absorbed by the tautomers at the excitation wavelength.)

Simultaneous measurements of the $H_2TPP-NO_2$ fluorescence kinetics and quantum yields in different solvents (Table 2) allow us to follow the influence of the solvent polarity on the radiative ($k_{rad}$) and nonradiative ($k_{nr}$) rate constants. Since two tautomers with different lifetimes $\tau_1$ and $\tau_2$ contribute to the fluorescence, the average lifetime $\tau_{av} = A_1\tau_1 + A_2\tau_2$ will be used. The calculations of $k_{rad} = \Phi_f/\tau_{av}$ and $k_{nr} = 1/\tau_{av} - k_{rad}$ result in the conclusion that $k_{rad}$ remains approximately constant for all the solvents used and equals $(3.5 \pm 0.6) \times 10^7$ $s^{-1}$, whereas $k_{nr}$ systematically decreases with an increase of $E_TN$, from $2.5 \times 10^8$ $s^{-1}$ for *n*-hexane to $1.1 \times 10^9$ $s^{-1}$ for DMF. The invariance of $k_{rad}$ shows that it is unlikely that the nature of the fluorescent state changes with an increase of the solvent polarity.

Taking into account that the quantum yield for triplet state formation, $\Phi_T \approx 0.4$ in DMF and $\Phi_T \approx 0.65$ in toluene, we can qualitatively evaluate which nonradiative pathway, internal conversion (rate constant $k_{ic}$) or intersystem crossing (rate constant $k_{isc}$) is responsible for the fluorescence lifetime shortening observed with an increase of the solvent polarity. Using the expressions $k_{isc} = \Phi_T/\tau_{av}$ and $k_{ic} = (1 - \Phi_T - \Phi_f)/\tau_{av}$, we conclude that $k_{isc} = 2.5 \times 10^8$ $s^{-1}$ in toluene and $k_{isc} = 4.4 \times 10^8$ $s^{-1}$ in DMF, whereas $k_{ic} = 1.0 \times 10^8$ $s^{-1}$ in toluene and $k_{ic} = 6.3 \times 10^8$ $s^{-1}$ in DMF. Therefore, both nonradiative pathways contribute to the fluorescence lifetime shortening, but the relative rise of the $k_{ic}$ with an increase of the solvent polarity is higher than that of $k_{isc}$.

*On the Nature of the Fluorescent State.* Useful information on the nature of the lowest excited singlet state of $H_2TPP-NO_2$ may be obtained from the analysis of the $S_1 \rightarrow S_n$ absorption spectrum. Indeed, if the $S_1$ state has full CT character, then the characteristic features of the porphyrin π-cation radical should be observed in the $S_1 \rightarrow S_n$ absorption spectrum. Such features have been observed, for example, for porphyrin−quinone dyads,[4] and these features primarily give rise to the presence of a broad intensive absorption band around 650−700 nm and the absence of the characteristic stimulated emission in the region of the fluorescence bands. None of these features were found in our case (Figure 9). By contrast, the observed $S_1 \rightarrow S_n$ absorption spectrum is a typical porphyrinic $^1(\pi,\pi^*)$ absorption spectrum. Somewhat unusual in this

spectrum is that the dips, which correspond to the ground-state absorption bands, are not very deep and do not come down to the negative $\Delta A$ region, as is usual for the "normal" porphyrins.[31] This can be easily explained because the extinction coefficients of the absorption maxima in the visible wavelength region are approximately twice as small for $H_2TPP-NO_2$ as compared to those of the "normal" porphyrin $H_2TPP$, owing to the strong inhomogeneous broadening in the first case, whereas the extinction coefficients of the extremely broad $S_1 \rightarrow S_n$ absorption band should be approximately equal for both molecules.

Therefore, it may be concluded from our results that the fluorescent state of $H_2TPP-NO_2$ is essentially a normal porphyrinic $^1(\pi,\pi^*)$ state that has a large dipole moment and exhibits a large conformational flexibility of the $NO_2$ group as a result of rotation around the C−N bond. The marked broadening and large Stokes shift of the fluorescence spectrum originate, most likely, from (1) the broad distribution of the $S_1$ state population with respect to the angle $\theta$ between the $NO_2$ and porphyrin planes and (2) the shift of this distribution to the side of smaller $\theta$ values as compared to the ground-state distribution. Therefore, an excitation of $H_2TPP-NO_2$ to the $S_1$ state most likely results in a more coplanar geometry of the $NO_2$ group relative to the porphyrin plane, with the $S_1$ state remaining essentially of $^1(\pi,\pi^*)$ character. A similar explanation was recently proposed to account for the unusual broadening of the fluorescence spectrum of the cationic free base tetrakis-(4-*N*-methylpyridyl)porphyrin in water.[39] In contrast to this, the TICT state formation, suggested in refs 7, 9, and 10 as a possible reason of the unusual fluorescence properties of the $\beta$-nitro-substituted tetraarylporphyrins, is inconsistent with our data because the TICT state should be characterized by (1) full electron transfer from the porphyrin ring to the $NO_2$ group and (2) orthogonal geometry of the $NO_2$ group with respect to the porphyrin macrocycle.[40,41]

**Acknowledgment.** This material is based upon work supported by the U.S. Civilian Research and Development Foundation under Award No. BC1-105. V.S.C. expresses his gratitude to the Wageningen Agriculture University for a Research Fellowship. We acknowledge use of the picosecond transient absorption spectrometer in the Institute of Physical Chemistry, Polish Academy of Sciences, and we are grateful to Dr. J. Dobkowski and V. A. Galievsky for the picosecond transient absorption measurements. We are also grateful to Dr. S. M. Bachilo for helpful and stimulating discussions.

## References and Notes

(1) Boxer, S. G. *Biochim. Biophys. Acta* **1983**, *726*, 265.
(2) Connolly, J. S.; Bolton, J. R. In *Photoinduced Electron Transfer*; Fox, M. A., Channon, M., Eds.; Elsevier: Amsterdam, 1988; Part D, Chapter 6.2, pp 303−393.
(3) (a) Gust, D.; Moore, T. A. *Science* **1989**, *244*, 35. (b) Gust, D.; Moore, T. A. *Adv. Photochem.* **1991**, *16*, 1. (c) Gust, D.; Moore, T. A. *Acc. Chem. Res.* **1993**, *26*, 198.
(4) Rodriguez, J.; Kirmaier, K.; Johnson, M. R.; Friesner, R. A.; Holten, D.; Sessler, J. L. *J. Am. Chem. Soc*. **1991**, *113*, 1652.
(5) Moore, T. A.; Gust, D.; Mathis, P.; Mialocq, J.-C.; Chachaty, C.; Bensasson, R. V.; Land, E. J.; Doizi, D.; Liddell, P. A.; Lehman, W. R.; Nemeth, G. A.; Moore, A. L. *Nature (London)* **1984**, *307*, 630.
(6) Tan, Q.; Kuciauskas, D.; Su, L.; Stone, S.; Moore, A. L.; Moore, T. A.; Gust, D. *J. Phys. Chem. B* **1997**, *101*, 5214.
(7) Gust, T. A.; Moore, D. K.; Luttrull, G. R.; Seely, E.; Bittersmann, R. V.; Bensasson, M.; Rugée, E. J.; Land., F. C.; De Schryver, M.; Van der Auweraer, M. *Photochem. Photobiol.* **1990**, *51*, 419.
(8) Takahashi, S.; Hase, T.; Komura, H.; Imanaga, O.; Ohno. *Bull. Chem. Soc. Jpn.* **1992**, *65*, 1475.
(9) Dahal, S.; Krishnan, V. *J. Photochem. Photobiol., A* **1995**, *89*, 105.
(10) Dahal, S.; Krishnan, V. *Chem. Phys. Lett.* **1997**, *274*, 390.
(11) Crossley, M. J.; Harding, M, M.; Sternhell, S. *J. Am. Chem. Soc.* **1986**, *108*, 3608.
(12) Crossley, M. J.; Field, L. D.; Harding, M. M.; Sternhell, S. *J. Am. Chem. Soc.* **1987**, *109*, 2335.
(13) Crossley, M. J.; Harding, M. M.; Sternhell, S. *J. Am. Chem. Soc.* **1992**, *114*, 3266.
(14) Little, R. G.; Anton, J. A.; Loach, P. A.; Ibers, J. A. *J. Heterocycl. Chem*. **1975**, *12*, 343.
(15) Baldwin, M. J.; Crossley, J. F.; DeBernardis, J. F. *Tetrahedron* **1982**, *38*, 685.
(16) Bruggeman, Y. E.; Boogert, A.; Van Hoek, A.; Jones, P. T.; Winter, G.; Schots, A.; Hilhorst, R. *FEBS Lett*. **1996**, *388*, 242.
(17) Van Hoek, A.; Visser, A. J. W. G. *Rev. Sci. Instrum*. **1981**, *52*, 1199.
(18) Van Hoek, A.; Visser, A. J. W. G. *Anal. Instrum*. **1985**, *14*, 359.
(19) Vos, K.; Van Hoek, A.; Visser, A. J. W. G. *Eur. J. Biochem*. **1987**, *165*, 55.
(20) Brochon, J. C. *Methods Enzymol.* **1994**, *240*, 262.
(21) Beechem, J. M.; Gratton, E.; Ameloot, M.; Knutson, J. R.; Brand, L. In *Topics in Fluorescence Spectroscopy* Lakowicz, J. R., Ed.; Plenum: New York, 1991; Vol. 2.
(22) Dobkowski, J.; Grabowski, Z. R.; Jasny, J.; Zielinski, Z. *Acta Phys. Pol., A* **1995**, *88*, 445.
(23) Stewart, J. J. P. *J. Comput. Chem*. **1991**, *12*, 320.
(24) Ridley, J.; Zerner, M. C. *Theor. Chim. Acta* **1973**, *32*, 111.
(25) Ridley, J.; Zerner, M. C. *Theor. Chim. Acta* **1976**, *42*, 223.
(26) Zerner, M. C.; Loew, G. H.; Kirchner, R. F.; Mueller-Westerhoff, U. T. *J. Am. Chem. Soc*. **1980**, *102*, 589.
(27) Reichardt, C. *Solvents and solvent effects in organic chemistry*; Mir: Moscow, 1991; Chapter 7, pp 524−530.
(28) Egorova, G. D.; Knyukshto, V. N.; Solov'ev, K. N.; Tsvirko, M. P. *Opt. Spektrosk.* **1980**, *48*, 1101.
(29) Bonnett, R. D.; McGarvey, D. J.; Harriman, A.; Land, E. J.; Truscott, T. G.; Winfield, U.-J. *Photochem. Photobiol.* **1988**, *48*, 271.
(30) Gradyushko, A. T.; Tsvirko, M. P. *Opt. Spektrosk.* **1971**, *31*, 291.
(31) Rodrigues, J.; Kirmaer, C.; Holten, D. *J. Am. Chem. Soc*. **1989**, *111*, 6500.
(32) Kuzmitsky, V. A.; Solovyov, K. N.; Tsvirko, M. P. In *Porphyrins: Spectroscopy, Electrochemistry, Applications*; Nauka: Moscow, 1987; pp 7−126 (in Russian).
(33) Gouterman, M. *J. Mol. Spectrosc*. **1961**, *6*, 138.
(34) Al-Hassan, K. A.; Rettig, W. *Chem. Phys. Lett.* **1986**, *126*, 273.
(35) Al-Hassan, K. A.; El-Bayoumi, M. A. *Chem. Phys. Lett*. **1986**, *123*, 39.
(36) Zenkevich, E. I.; Shulga, A. M.; Chernook, A. V.; Gurinovich, G. P.; Sagun, E. I. *J. Appl. Spectrosc.* **1985**, *42*, 772.
(37) Zenkevich, E. I.; Shulga, A. M.; Filatov, I. V.; Chernook, A. V.; Gurinovich, G. P. *Chem. Phys. Lett*. **1985**, *120*, 63.
(38) Zenkevich, E. I.; Shulga, A. M.; Chernook, A. V.; Gurinovich, G. P. *Chem. Phys. Lett*. **1984**, *109*, 306.
(39) Vergeldt, F. J.; Koehorst, R. B.; van Hoek, A.; Schaafsma, T. J. *J. Phys. Chem*. **1995**, *99*, 4397.
(40) Grabowski, Z. R.; Rotkiewicz, K.; Siemiarczuk, A.; Cowley, D. J.; Baumann, W. *Nouv. J. Chim*. **1979**, *3*, 443.
(41) Rettig, W. In *Topics in Current Chemistry*; Springer-Verlag: Berlin, Heidelberg, 1994; Vol. 169, pp 254−299.